Episodic reservoir flooding transforming sediment sinks to sources and the potential global implications

Check for updates

Haifei Yang [1], Min Tian[1], Shilun Yang [1] ✉, Benwei Shi[1], Chunpeng Chen[1] & Houjie Wang[2,3]

Reservoirs are widely recognized as sediment sinks, but the role of silted-up reservoirs as sediment sources remains poorly understood. This study presents quantitative assessments on episodic erosion effects of reservoirs in the Yellow River. Here we showed that sediment erosion during the 2019 flooding was 112 and 265 million tons at the Sanmenxia and Xiaolangdi reservoirs, respectively. Nearly all the Sanmenxia erosion was attributable to natural floods, whereas only ~40% of the Xiaolangdi erosion resulted from natural floods with the rest from drawdown and artificial flooding. These erosions contributed ~1/4 of decadal fluvial sediment flux. Reservoir erosion increased downstream suspended sediment concentration by over two orders of magnitude. Threshold siltation ratios (sedimentation volume/storage capacity) for initial erosion in the studied reservoirs ranged from 28% to 87%, averaging 60% ± 21%. Considering many reservoirs experiencing >30% capacity loss and intensifying floods under global warming, reservoir erosion will become more frequent worldwide.

Dams have been constructed on most of the world's large and moderate rivers, and the impacts of reservoirs on rivers, deltas, and adjacent seas have been extensively studied in recent decades[1–6]. The retention of sediment in reservoirs and sediment deficits in downstream channels and deltas are among the most important environmental impacts of dam construction. In extreme cases, such as the Nile (Egypt), Colorado (Mexico), and Kizil Irmak (Turkey) rivers, the sediment flux to the sea has decreased to almost zero[7,8]. Dam construction on the Yellow, Yangtze, Pearl, and Liao rivers of China; the Narmada and Krishna rivers of India; the Mississippi and Rio Grande rivers of the USA; and the Indus (Pakistan), Red (Vietnam), Chao Phraya (Thailand), Orange (South Africa), Limpopo (Mozambique), Volta (Ghana), Rhone (France), Ebro (Spain), Yenisei (Russia), and Ombrone (Italy) rivers has led to 50–95% reductions in sediment discharge[2,9–13]. Furthermore, sediment retention in reservoirs has resulted in downstream channels and deltas being degraded[14–19].

In contrast to the numerous studies of reservoir-induced long-term downstream sediment reduction and morphological degradation, less is understood of the impact of episodic reservoir erosion on fluvial sediment loads and channel–delta stability. Scouring events in small reservoirs and the consequent downstream sediment pulses associated with dam removal or breaching (partial removal) and hydraulic flushing have been documented[20–25], but it remains unclear whether episodic erosion also occurs from large (storage capacity >0.1 km³) silted-up in-use

reservoirs during flooding or due to the combined effects of flooding and drawdown, and how such episodic erosion affects downstream sediment transport and morphodynamics. Quantitative assessment of sediment budgets between reservoir erosion and downstream sediment delivery and deposition is particularly lacking. Many reservoirs constructed worldwide over the last 150 years are highly silted-up[2,7,9,12,26–30]. Many new reservoirs are currently under construction or in the planning stage, particularly in developing countries[5,31]. As more reservoirs silt up, the increasing frequency and intensity of extreme precipitation events due to global warming[32,33] necessitates investigation of whether episodic erosion is likely in silted-up reservoirs under natural or regulated conditions and its potential effects on downstream sediment delivery and morphodynamics.

Here, case studies, particularly on the Yellow River (Fig. 1), were employed to address the above questions with the aims of (1) quantitatively assessing episodic reservoir erosion and its effects on downstream sediment loads and channel deposition; (2) constructing a sediment budget for the reservoir-downstream-channel systems; (3) investigating natural and anthropogenic factors responsible for reservoir erosion events; and (4) providing an overview of the potential of episodic erosion in silted-up reservoirs worldwide. The results aim to enhance our understanding of the role of silted-up reservoirs as fluvial sediment sources under extreme hydrometeorological conditions and associated human impacts.

[1]State Key Laboratory of Estuarine and Coastal Research, East China Normal University, Shanghai, China. [2]Key Laboratory of Submarine Geosciences and Prospecting Techniques, College of Marine Geosciences, Ocean University of China, Qingdao, China. [3]Laboratory for Marine Geology, Qingdao National Laboratory for Marine Science and Technology, Qingdao, China. ✉e-mail: slyang@sklec.ecnu.edu.cn
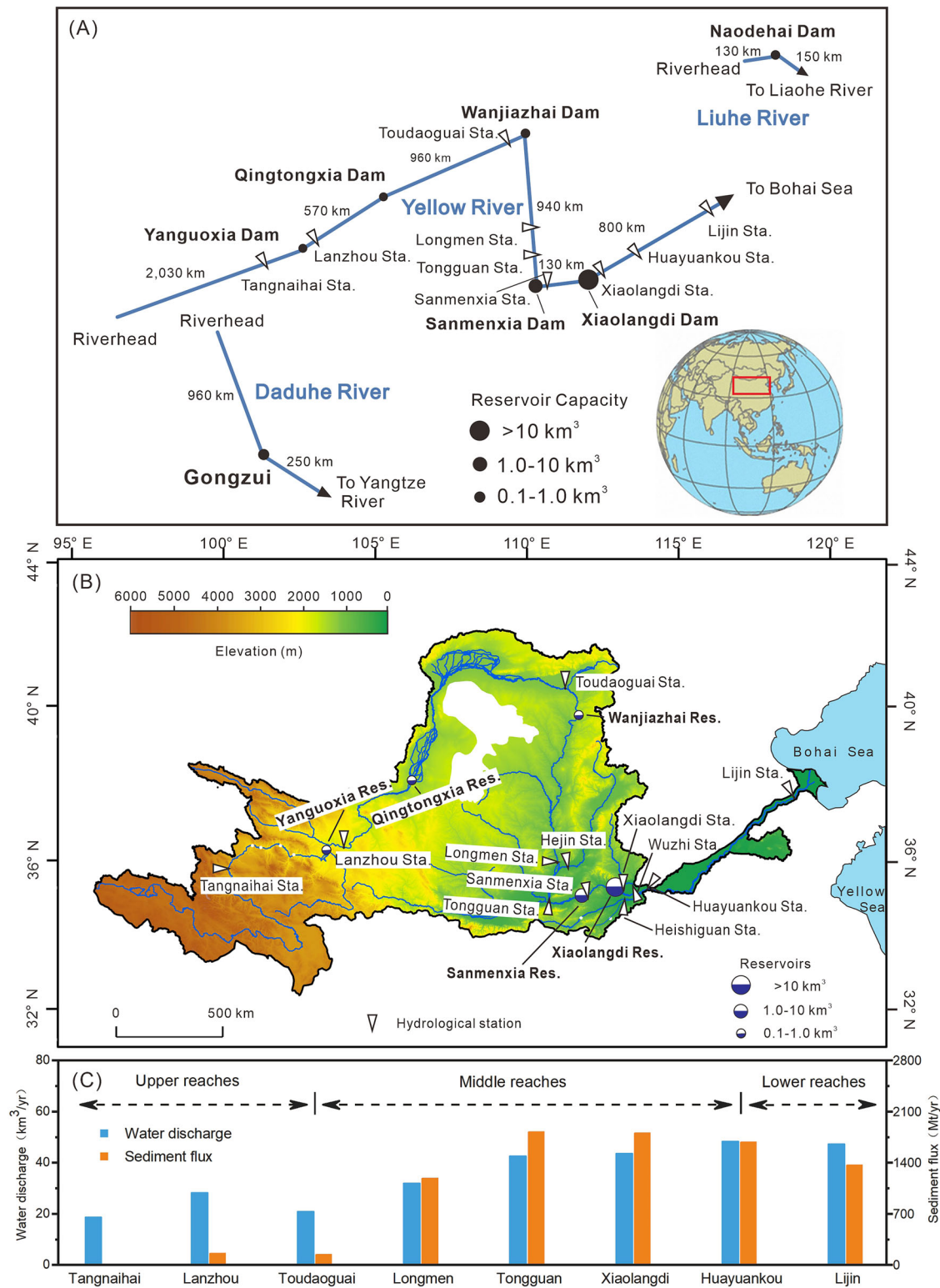
Fig. 1 | Diagrams showing the upstream and downstream reservoirs and hydrological stations in the study area. **A** Schematic diagram of the studied reservoirs. Dots indicate dam locations; lines represent general directions, rather than actual river channels. Distances in the river courses are shown. **B** Map of the Yellow River basin showing the locations of major reservoirs, gauging stations, and cities. **C** Multiyear average water and sediment fluxes at gauging stations along the mainstream of the Yellow River prior to reservoir construction (1952–1959).

Results
Erosion of the Xiaolangdi and Sanmenxia reservoirs and its downstream sedimentary and morphological impacts in a flood season

Runoff of the Yellow River during the 2019 flood season was much higher than normal. For example, the monthly water discharge at Sanmenxia Station in July–September 2019 (6090 Mm^3) was 2.5 times the multiyear average (2450 Mm^3) (Supplementary Fig. S1). Based on daily water inflows to the Sanmenxia and Xiaolangdi reservoirs, there were two major natural flood events. The maximum water inflows to the Sanmenxia Reservoir during the first and second flood events were 4850 and 4490 m^3 s^{-1},
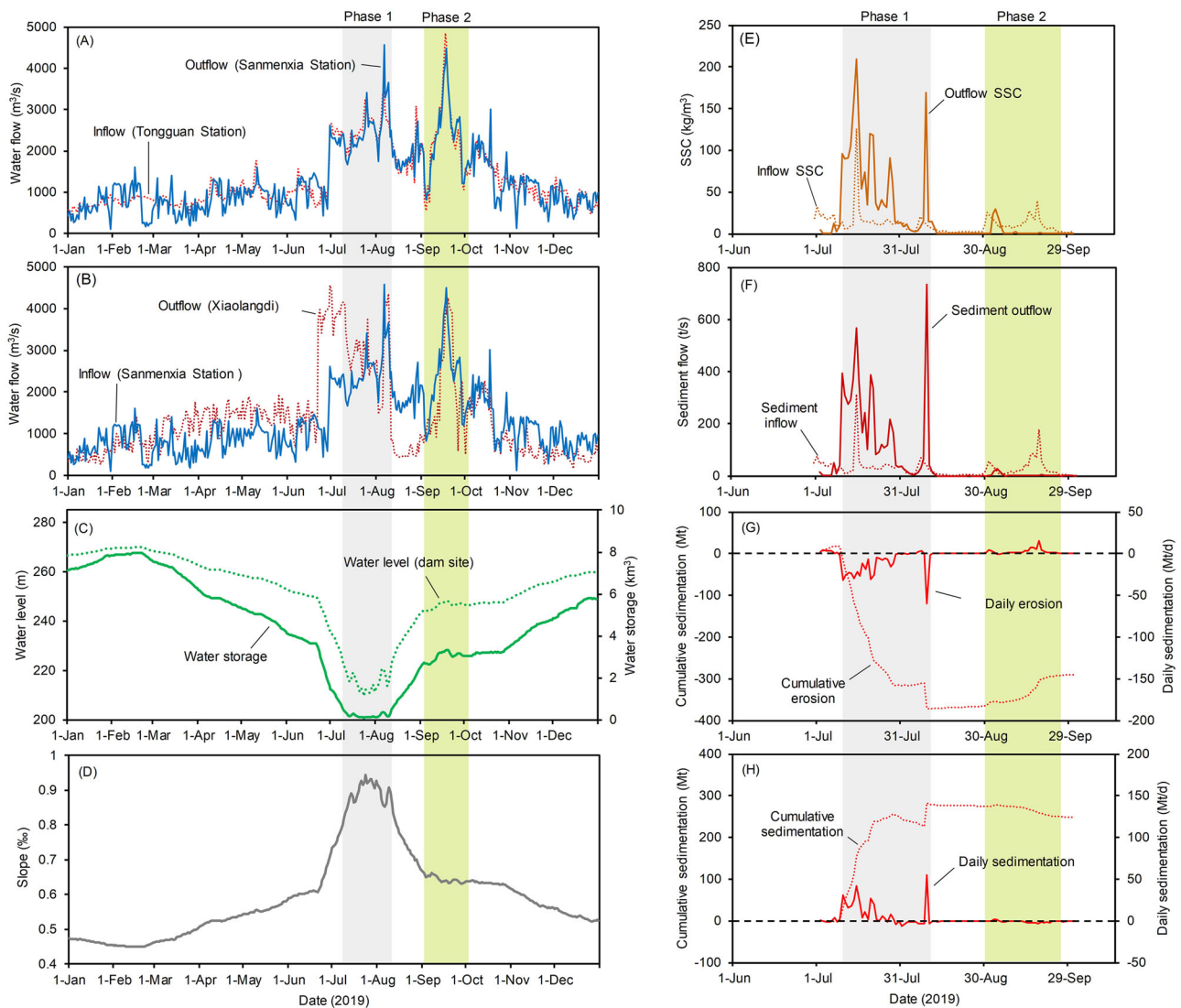
Fig. 2 | Temporal variations of water and sediment in the Sanmenxia and Xiaolangdi reservoirs. A Time series of daily water inflow and outflow for the Sanmenxia Reservoir. **B** Water inflow and outflow, **C** water level and storage, **D** water-surface slope, **E** inflow and outflow SSC, **F** sediment inflow and outflow, and **G** erosion and cumulative erosion for the Xiaolangdi Reservoir. **H** Sedimentation

and cumulative sedimentation in downstream reaches between Xiaolangdi and Huayuankou stations. Note: inflow to the Xiaolangdi Reservoir equals the outflow from the Sanmenxia Reservoir; daily inflow SSC data for the Sanmenxia Reservoir and daily inflow and outflow SSC data in January–June and October–December for the Xiaolangdi Reservoir are unavailable.

respectively, almost six times the water inflow during the dry season (averaging 780 m³ s⁻¹ from January to May). Water outflows from the Sanmenxia Reservoir were generally consistent with water inflows (Fig. 2A). However, there were notable differences between inflows and outflows at the Xiaolangdi Reservoir, where outflows were markedly higher than inflows from March to late July 2019, especially during the 20 days from 22 June to 11 July (Fig. 2B). During this period, the water level decreased by ~60 m and water storage decreased to nearly zero from ~8 km³ (Fig. 2C), with a doubling of water-surface slope (Fig. 2D).

During the period of 9 July–10 August (Phase 1, Fig. 2), the water flow through the Xiaolangdi Reservoir was unusually high (Fig. 2B) while the water level was the lowest (Fig. 2C) and the water gradient was the largest (Fig. 2D). As a result, the suspended sediment concentration (SSC) of the Xiaolangdi Reservoir outflow increased markedly despite fluctuations, and was notably higher than the inflow SSC. The highest outflow SSC of 210 kg m⁻³ was observed in the initial stage of Phase 1 (15 July) when inflow and outflow were 2500 and 2,720 m³ s⁻¹, respectively. The second highest outflow SSC of 170 kg m⁻³ was observed at the end of Phase 1 (9 August) when the inflow was 3,660 m³ s⁻¹ and the outflow increased rapidly to its

second highest level of 4,350 m³ s⁻¹ after a brief reduction. During this Phase 1 period, the mean outflow SSC of 57 kg m⁻³ was 3.8 times that of the mean inflow SSC (15 kg m⁻³), and the maximum ratio of daily outflow to inflow SSC reached 17 (Fig. 2E).

The sediment outflow increased with a trend similar to that of the outflow SSC and peaked at the end of Phase 1, whereas the second-highest outflow occurred in the initial stage of Phase 1 (Fig. 2F). Considering the difference between sediment outflow and inflow, the erosion rate peaked at 60 Mt d⁻¹ (Mt: million tons) (693 t s⁻¹) on 9 August, at up to 17 times the sediment inflow (41 t s⁻¹), accounting for 94% of the daily sediment outflow of 735 t s⁻¹. The second highest erosion rate of 31 Mt d⁻¹ (362 t s⁻¹) occurred in the initial stage of Phase 1 (July 10), at 12 times the sediment inflow (30 t s⁻¹), contributing 92% of the sediment outflow of 392 t s⁻¹. The cumulative erosion in the Xiaolangdi Reservoir during the one month of Phase 1 reached 373 Mt, or 3.4 times the cumulative sediment inflow (109 Mt), contributing 74% of the cumulative sediment outflow of 498 Mt (Fig. 2F–G). At Xiaolangdi Station, the annual sediment flux in 2019 was 545 Mt, and the cumulative sediment flux for 2010–2019 was 1566 Mt. Erosion in the Xiaolangdi Reservoir during the flood event of July 2019 thus contributed

68% of the annual sediment flux and 24% of the decadal sediment flux in downstream channels.

After this rapid erosion, the Xiaolangdi Reservoir experienced a period of balanced sedimentation and erosion (10–31 August), when water outflow decreased more rapidly than inflow, and the water slope decreased to half its maximum value due to water impoundment (Fig. 2B–D). Another flood occurred in the Yellow River in September 2019 (Phase 2), during which water outflow from the Xiaolangdi Reservoir was consistent with inflow, and the inflow SSC was markedly higher than outflow SSC. In this second flood event, the sediment outflow from the Sanmenxia Reservoir (i.e., the sediment inflow to the Xiaolangdi Reservoir) was ~80 Mt, while the outflow from the Xiaolangdi Reservoir was ~10 Mt, resulting in sedimentation of ~70 Mt in the Xiaolangdi Reservoir (Fig. 2).

The absence of direct SSC inflow data for the Sanmenxia Reservoir precluded an estimation of daily sedimentation and erosion, but the three major peaks in outflow SSC (i.e., inflow SSC to the Xiaolangdi Reservoir) likely indicate erosion events in the Sanmenxia Reservoir (Fig. 2E). The first outflow SSC peak of 32 kg m^{-3} (compared to <1 kg m^{-3} under normal conditions) occurred on 1 July (Fig. 2E) when water inflow and outflow of the Sanmenxia Reservoir were 2660 and 2330 m^3 s^{-1}, respectively. These high flows were derived from the first flood event in the river basin. During 28–30 June, the water inflow increased from 735 to 2,620 m^3 s^{-1}, and outflow from 589 to 2,620 m^3 s^{-1} (Fig. 2A). The outflow SSC from the Sanmenxia Reservoir was 18.8 kg m^{-3} on 30 June (earlier SSC data were unavailable) (Fig. 2E). The second outflow SSC peak of 126 kg m^{-3} occurred on 15 July, when Sanmenxia Reservoir inflow and outflow were 2370 and 2500 m^3 s^{-1}, respectively, following a temporary reduction. The third peak of 40 kg m^{-3} occurred on 18 September, when Sanmenxia Reservoir inflow and outflow were 4650 and 4490 m^3 s^{-1}, respectively (Fig. 2A, E). Rapid erosion in the Sanmenxia Reservoir during the 2019 flood season is corroborated by annual sediment load data issued by the Ministry of Water Resources of China[34].

River channels downstream of the Xiaolangdi Reservoir exhibited opposing reactions to the rapid erosion occurring in the reservoir. Prior to the flood events, the river water in the downstream channel of the Xiaolangdi Reservoir was clear (Fig. 3A); during the flood events, a large amount of sediment poured down from the Xiaolangdi Reservoir, resulting in a rapid increase in SSC in the downstream channel (Fig. 3B, C); after the flood events, the downstream channel returned to a low SSC state (Fig. 3D). During the flood events, cumulative sedimentation in the 126 km length of downstream channels between Xiaolangdi and Huayuankou stations reached ~280 Mt, which accounted for 75% of the Xiaolangdi Reservoir erosion (373 Mt). The date of maximum daily sedimentation in the downstream channels (9 August, 55 Mt) was consistent with that of maximum daily Xiaolangdi Reservoir erosion (9 August, 60 Mt) (Fig. 2H).

Annual deposition and erosion in the seven reservoirs over the past decades

The annual water and sediment supplies from the gauged and ungauged areas all showed rapid decreasing trends over the past seven decades (Supplementary Fig. S2). The water discharges at the Tongguan Station (entrance of the Sanmenxia Reservoir) ranged from 14.9 to 69.9 km^3 yr^{-1}, and averaged 33.4 km^3 yr^{-1}; the sediment fluxes at the Tongguan Station ranged from 55 to 2995 Mt yr^{-1} and averaged 911 Mt yr^{-1}. The estimated water discharges from the ungauged areas between Tongguan station and Xiaolangdi Station (immediately downstream of the Xiaolangdi Dam) ranged from 0.17 to 2.70 km^3 yr^{-1}, and averaged 0.72 km^3 yr^{-1}; the estimated sediment fluxes from the ungauged areas between Tongguan station and Xiaolangdi Station ranged from 0.05 to 44.5 Mt yr^{-1}, and averaged 5.6 Mt yr^{-1}. The total annual water inflows of the Sanmenxia and Xiaolangdi reservoirs (defined as sum of the water discharge at the Tongguan Station and the water supply from the ungauged areas) ranged from 15.2 to 72.6 km^3 yr^{-1}, and averaged 34.1 km^3 yr^{-1}; the total annual sediment inflows of the Sanmenxia and Xiaolangdi reservoirs (defined as sum of the sediment flux at the Tongguan Station and the sediment supply from the ungauged areas)

ranged from 55.1 to 3034 Mt yr^{-1}, and averaged 916 Mt yr^{-1}. The contribution of the ungauged water discharge to the total water inflow into the reservoirs ranged from 0.63% to 4.67%, and averaged 2.04%; the contribution of the ungauged sediment supply to the total sediment inflow into the reservoirs ranged from 0.01% to 1.64% and averaged 0.39%. Thus, the contribution of the ungauged water and sediment supply to the water and sediment flows of the reservoirs were generally low. At the Xiaolangdi Station, the water discharge ranged from 14.4 to 70.2 km^3 yr^{-1} and averaged 33.6 km^3 yr^{-1}; the sediment flux ranged from ~1 to 2980 Mt yr^{-1} and averaged 837 Mt yr^{-1}. The absolute predominance of gauged sediment flux over ungauged sediment supply suggests that annual depositions and erosions of the Sanmenxia and Xiaolangdi reservoirs based on sediment budget are highly reliable.

Based on annual sediment inflow and outflow data, the net erosion of the Xiaolangdi Reservoir in 2019 was 265 Mt (Fig. 4). The net erosion in this reservoir during July–September 2019 was ~300 Mt (Fig. 2G), indicating a cumulative sedimentation of ~35 Mt during the remaining nine months of that year when daily sediment-load data were unavailable. The sediment inflow and outflow of the Sanmenxia Reservoir in 2019 were 168 and 280 Mt, respectively, indicating an annual net erosion of ~112 Mt, with most occurring during the flood events when >85% of the annual sediment outflow from the Sanmenxia Reservoir (i.e., sediment inflow to the Xiaolangdi Reservoir) occurred during the flood season (July–September) (Fig. 2F).

Initial erosion in the Sanmenxia Reservoir was recorded in 1965, only five years after impoundment, with the initial annual erosion of 277 Mt yr^{-1} contributing almost 40% of the downstream annual sediment load (735 Mt yr^{-1}). The highest annual erosion of 300 Mt was recorded in 1971 (Fig. 4), contributing 18% of the downstream sediment load (1650 Mt). In 2020, Sanmenxia Reservoir erosion (104 Mt) contributed 30% of the downstream sediment load of 344 Mt. In the period 1965–2020, erosion exceeded sedimentation in the Sanmenxia Reservoir, with a cumulative erosion of 1430 Mt (735 Mt yr^{-1}), with yearly alternations between erosion and deposition. More than 40% of the total sedimentation of 1960–1964 (3480 Mt) was eroded in the following 55 years.

For the Xiaolangdi Reservoir, prior to erosion in 2019, sedimentation was continuous for 20 years (1999–2018), with a cumulative sedimentation of 3260 Mt (163 Mt yr^{-1}; Fig. 4). The overall dry bulk density of the rapid sedimentation in the Sanmenxia and Xiaolangdi reservoirs was 0.93 g cm^{-3} (Supplementary Fig. S3), giving sedimentation volumes in the Sanmenxia Reservoir (1960–1964) and Xiaolangdi Reservoir (1999–2018) of 3.74 and 3.50 km^3, respectively. The storage capacities of the Sanmenxia and Xiaolangdi reservoirs were 6.0 and 12.7 km^3, and their initial net annual erosion occurred at the time when siltation-induced storage capacity losses were 62% and 28%, respectively.

Annual net erosion events have also been recorded for the Qingtongxia, Yanguoxia, Wanjiazhai, Naodehai, and Gongzui reservoirs (Fig. 5). Initial erosion in these reservoirs occurred 5–26 years after impoundment, when cumulative losses of storage capacity due to previous sedimentation were 43–87% (Table 1). The Qingtongxia Reservoir began operation in 1967, with initial erosion occurring in 1972, when the cumulative storage capacity loss due to rapid sedimentation was 87% (average 105 Mm^3 yr^{-1}). The highest annual erosion recorded in the Qingtongxia Reservoir was 28 Mm^3 yr^{-1} in 1981, with a maximum relative increase in annual sediment outflow of 40% (Fig. 5A; Table 1). The Yanguoxia Reservoir began operation in 1961, with initial erosion in 1971 when the cumulative storage capacity loss due to sedimentation was 76% (average 18 Mm^3 yr^{-1}). The highest annual erosion recorded in the Yanguoxia Reservoir was 6.1 Mm^3 in 1971, with a maximum relative increase in the annual sediment outflow of 52% (Fig. 5B; Table 1). The Wanjiazhai Reservoir began operation in 1998, with initial erosion in 2014 when the cumulative loss of storage capacity due to sedimentation was 50% (average 28 Mm^3 yr^{-1}). The highest annual erosion recorded in the Wanjiazhai Reservoir was 7.6 Mm^3 in 2014, with a maximum relative increase in annual sediment outflow of 49% (Fig. 5C; Table 1). The Naodehai Reservoir began operation in 1942, with initial erosion in

Fig. 3 | Changes in turbidity in the downstream channel of Xiaolangdi Reservoir. River channel conditions **A** Before, **B**, **C** during, and **D** after Flood Period 1 (Phase 1 in Fig. 2).
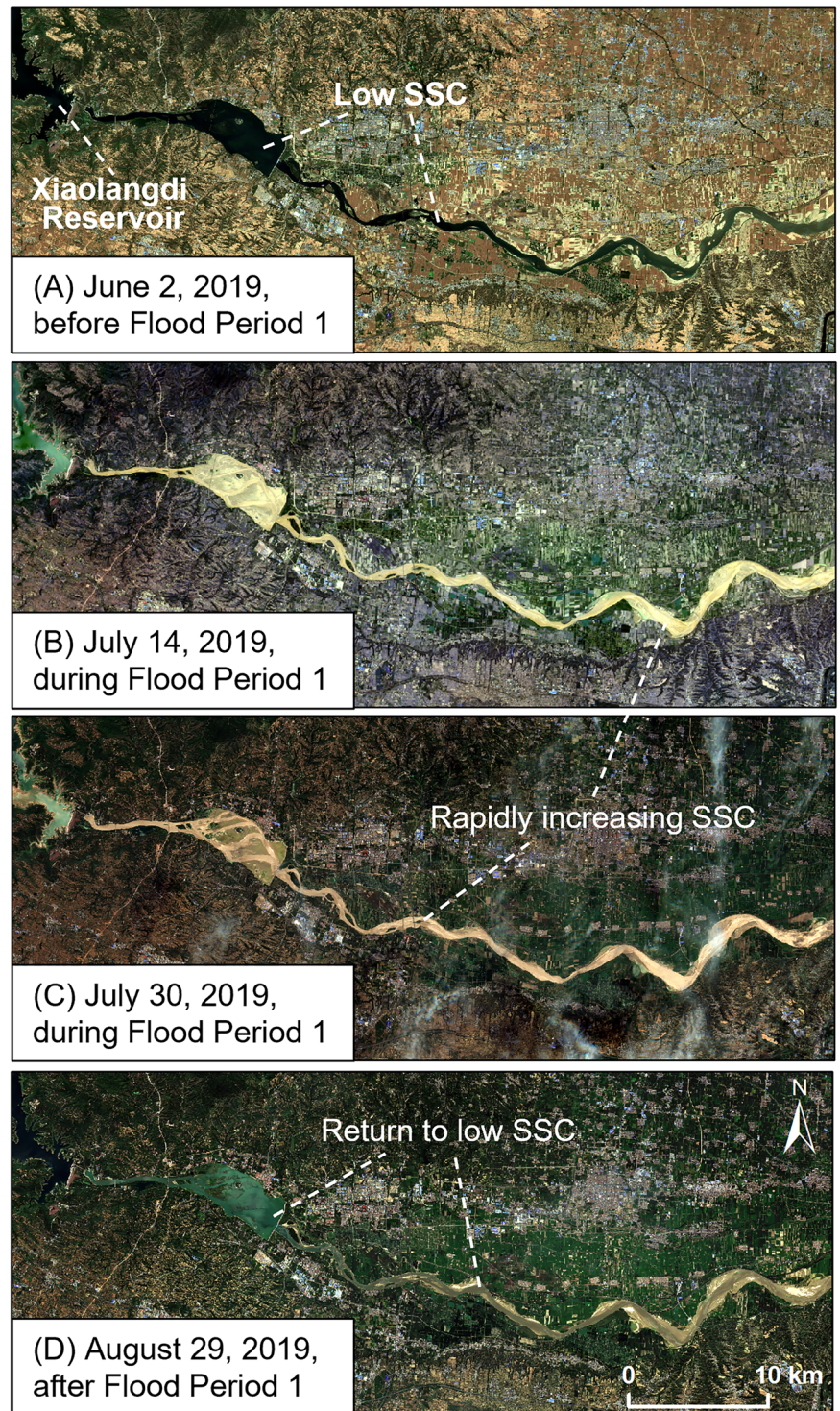
1951 when the cumulative loss of storage capacity due to sedimentation was 43% (average 8 Mm³ yr⁻¹). The highest annual erosion recorded in the Naodehai Reservoir was 8.8 Mm³ in 1965, with a maximum relative increase in the annual sediment outflow of 59% (Fig. 5D; Table 1). The Gongzui Reservoir began operation in 1971, with initial erosion in 1987 when the cumulative loss of storage capacity due to sedimentation was 71% (average 14 Mm³ yr⁻¹). The highest annual erosion recorded in the Gongzui Reservoir was 3.1 Mm³ in 2000, with a maximum relative increase in annual sediment outflow of 11% (Fig. 5E; Table 1). After the initial erosion events, storage capacities of the reservoirs tended to stabilize even though deposition and erosion occurred alternately (Fig. 5).

Deposition thickness in 1999–2018 and erosion depth in 2019 in the Xiaolangdi Reservoir

For the Xiaolangdi Reservoir, deposition during 1999–2018 and erosion during 2019 occurred mainly in the mainstream channel. Along the 120-km length of thalweg, the mean thickness of deposited sediment during 1999–2018 was 49 m (2.45 m yr⁻¹), with a maximum thickness of 77 m at sites located 5–10 km upstream of the dam. In 2019, the mean erosion depth along the thalweg was 7.3 m, with a maximum erosion depth of 11 m in the middle reaches of the main river channel (Fig. 6A). In the channel cross-section, deposition during 1999–2018 and erosion in 2019 occurred mainly in the deep channel, with little bathymetric change near the riverbanks
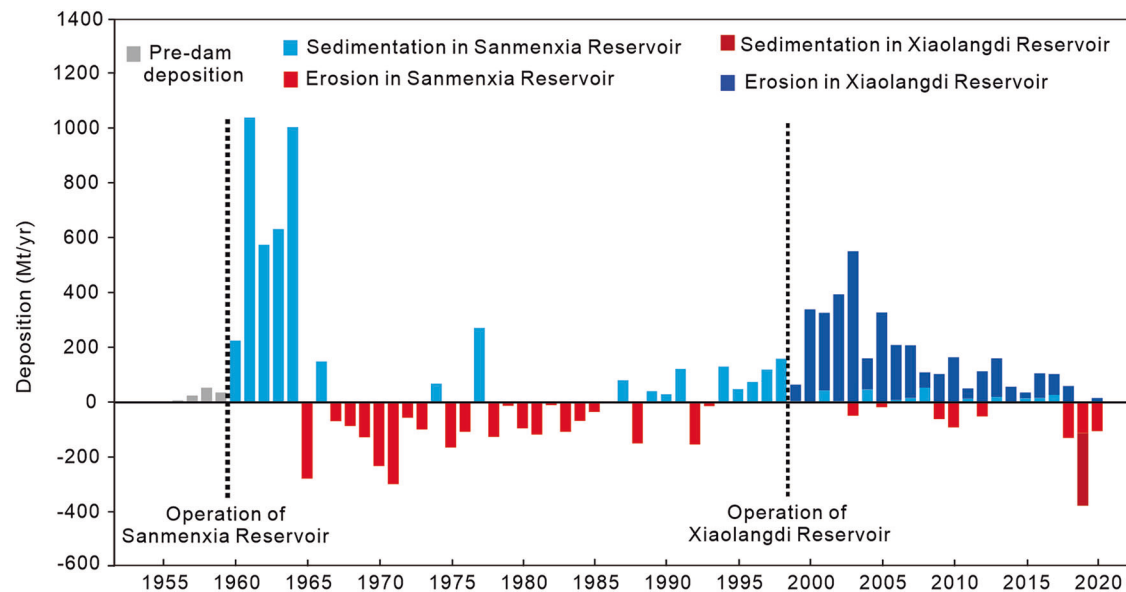
Fig. 4 | Annual sedimentation and erosion in the Sanmenxia Reservoir and Xiaolangdi Reservoir. Because the Sanmenxia and Xiaolangdi reservoirs began operation in 1960 and 1999, respectively, sedimentation and erosion are shown for only Sanmenxia Reservoir prior to 1999, whereas sedimentation and erosion are shown for both Sanmenxia and Xiaolangdi reservoirs since 1999.
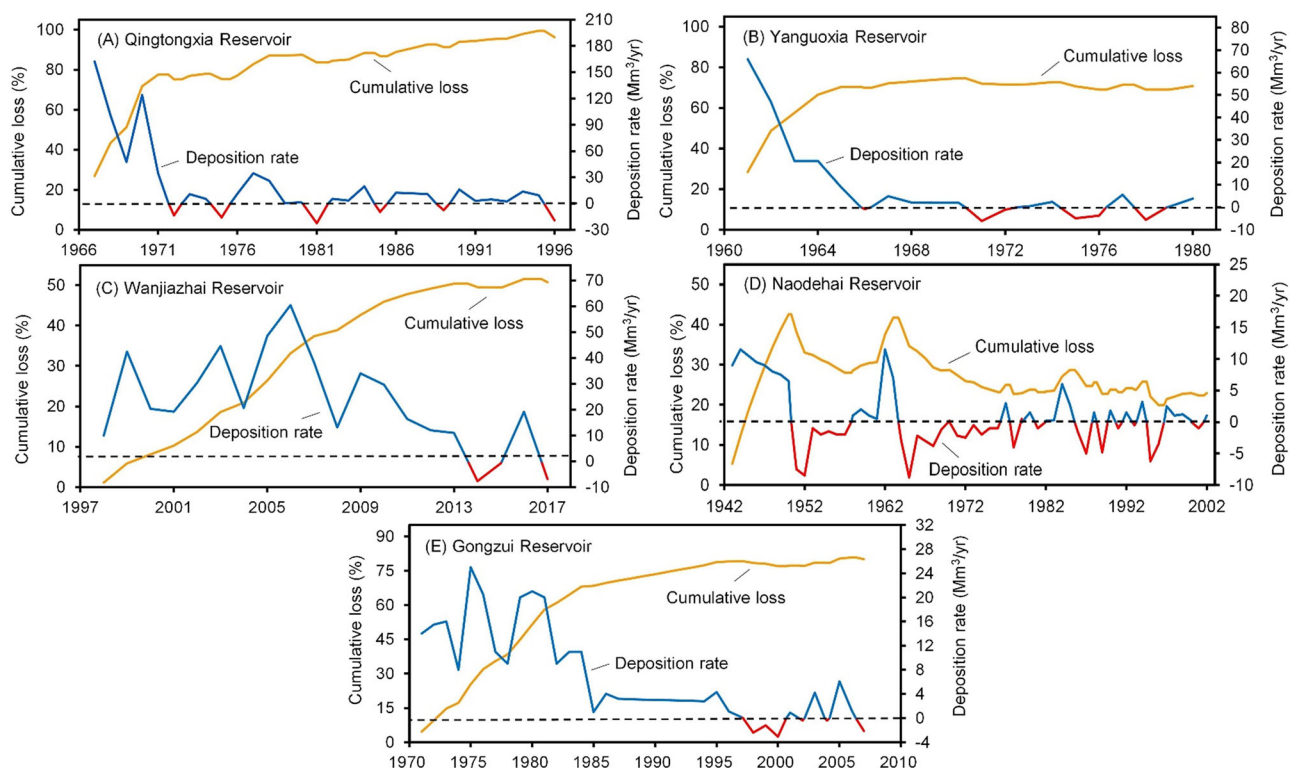

Fig. 5 | Annual deposition rate and cumulative loss of storage capacity in reservoirs. A–C Qingtongxia, Yanguoxia, and Wanjiazhai reservoirs in the upstream and upper middle reaches of the Yellow River (see Fig. 1A for locations). **D** Naodehai Reservoir on the Liuhe River, a tributary of the upper Liaohe River. **E** Gongzui Reservoir on the Daduhe River, a tributary of the upper Yangtze River.

Note: sources of deposition/erosion data were as follows: Qingtongxia Reservoir, changes in storage capacity reported by Li[67]; Yanguoxia Reservoir, Zhang[68]; Wanjiazhai Reservoir, Ren et al.[69]; Naodehai Reservoir, changes in storage capacity reported by Han[27] and Jiao et al.[63]; Gongzui Reservoir, Lin[65] for 1971–1986 and Xiong and Ma[70] for 1994–2007.

(Fig. 6B–C). This rapid erosion occurred mainly during the flood event of July 2019. Bathymetric surveys in the Xiaolangdi Reservoir were undertaken each October, and erosion in 2019 was based on bathymetric survey data of October 2018 and October 2019. Based on the data in Fig. 2G, the erosion depth in Fig. 6 would have resulted from episodic erosion during floods from July to early August 2019. More importantly, maximum erosion depths during the episodic events would have been greater than those shown in Fig. 6 due to the recovery of deposition in September 2019 (Fig. 2G).

Table 1 | Examples of reservoir erosion after years to decades of sedimentation, and impact on downstream sediment delivery

Reservoir	River	Storage capacity (Mm³)	Storage capacity loss prior to initial annual net erosion		Maximum erosion		Maximum impact on downstream sediment flux		Sediment inflow (Mt yr⁻¹)	Increased sediment outflow (%)
			Operation period	Loss (%)	Year	Erosion (Mm³ yr⁻¹)	Year	Erosion (Mt yr⁻¹)	Sediment inflow (Mt yr⁻¹)	Increased sediment outflow (%)
Sanmenxia[a]	Yellow	6000	1960–1964	62	1971	298	1965	277	455	61
Xiaolangdi	Yellow	12,700	1999–2018	28	2019	356	2019	356	180	198
Qingtongxia[b]	Yellow	607	1967–1971	87	1981	22	1975	21.4	53.5	40
Yanguoxia[c]	Yellow	232	1961–1970	76	1971	6.1	1975	6.75	13.0	52
Wanjiazhai[d]	Yellow	896	1998–2013	50	2014	7.6	2017	9.18	18.7	49
Naodehai[e]	Liuhe	168	1942–1950	43	1965	8.8	1965	11.9	20.2	59
Gongzui[f]	Daduhe	310	1971–1986	71	2000	3.1	2000	4.09	37.2	11

[a]The original storage capacity of the Sanmenxia Reservoir (below an elevation of 330 m from the semi-entrance at Tongguan Station) is from Lin[65]; erosion, sediment outflow, and dry bulk density for conversion from volume to weight of eroded deposits are based on Li[67] and Jia[73]. [b]Capacity loss and erosion are based on Zhang[66]; sediment outflow was measured by the YRCC at Lanzhou Station, immediately downstream of the Yanguoxia Reservoir. [c]Capacity loss and erosion are based on Ren et al.[69]; sediment outflow is the sum of reservoir erosion and sediment inflow (measured at Toudaoguai Station, immediately upstream of the Wanjiazhai Reservoir). [d]Original data are from Han[27] and Jiao et al.[63]. Dry bulk density in the Qingtongxia Reservoir was used for the Naodehai Reservoir because the natural conditions (climate, lithology, hydrology, elevation) and sedimentation history of the two reservoirs are similar. [e]Capacity loss is after Lin[65]. Erosion volume and sediment outflow are based on Xiong and Ma[70]. A frequently used dry bulk density for the Yangtze River sediments was adopted from Yang et al.[15] to calculate the weight of eroded sediments in the Gongzui Reservoir.

Impacts of annual deposition/erosion of the Sanmenxia and Xiaolangdi reservoirs on downstream sediment load and channel morphology

Slow net erosion (6 Mt yr⁻¹) occurred in the previously highly silted-up Sanmenxia Reservoir during 1999–2018, while rapid deposition (169 Mt yr⁻¹) occurred in the newly formed Xiaolangdi Reservoir. Most (62%) of the sediment from upstream reaches was retained in the Xiaolangdi Reservoir, which led to a dramatic decrease in sediment outflow and a sharp decline in downstream SSC levels, resulting in channel erosion in reaches downstream of the Xiaolangdi Reservoir. The total erosion rate in the 756 km of downstream reaches was 44 Mt yr⁻¹, offsetting ~25% of the sediment loss due to reservoir deposition. The erosion intensity in the first 126 km reach (0.09 Mt km⁻¹ yr⁻¹) was higher than that in the lower 630 km reach (0.05 Mt km⁻¹ yr⁻¹). Downstream sediment erosion occurred at a much lower rate than reservoir deposition, so sediment discharge to the sea was markedly reduced relative to the fluvial sediment load above the reservoirs (Fig. 7A).

In 2019, the total erosion in the Sanmenxia and Xiaolangdi reservoirs amounted to 377 Mt, which increased the downstream sediment load by 224%. As a result, rapid deposition occurred in channels downstream of the Xiaolangdi Dam: deposition rates were 228 Mt yr⁻¹ in the 126 km upper reaches (1.8 Mt km⁻¹ yr⁻¹) and 9 Mt yr⁻¹ in the 630 km middle–lower reaches (0.01 Mt km⁻¹ yr⁻¹) (Fig. 7B), showing a rapid downstream decreasing trend. Assuming all deposition was contributed by sediment derived from reservoir erosion, 63% of eroded sediment from the two reservoirs settled in downstream channels. This assumption is reasonable considering that deposition is unlikely to occur in these channels without an increased sediment supply from reservoir erosion (see Fig. 7A). Although most sediment derived from reservoir erosion was deposited in the downstream channels, the sediment discharge from the Yellow River to the Bohai Sea increased by 61% relative to the sediment load at the Tongguan Station above the reservoirs (Fig. 7B).

Discussion

In 2019, the time series of daily water outflow of the Sanmenxia Reservoir in 2019 was in good agreement with the time series of water inflow (Fig. 2A), suggesting that few water-level management practices were conducted in this reservoir in 2019. Thus, nearly all of the 112 Mt erosion of the Sanmenxia Reservoir in 2019 could be attributed to natural floods, whereas little erosion was attributable to drawdown and artificial floods. In contrast, considerable water drawdown was conducted in the Xiaolangdi Reservoir in 2019. In fact, more than 95% of the water storage was released from March to July (Fig. 2C). During this period, the water outflow of the Xiaolangdi Reservoir was evidently higher than the water inflow, suggesting an artificial flow in the reservoir. Most importantly, the water outflow was ~2 times higher than the water inflow from the end of June to mid-July, resulting from the combination of natural and artificial floods. Because water inflow of the Xiaolangdi Reservoir was almost equal to the water inflow of the Sanmenxia Reservoir, we roughly estimated that natural flood-induced erosion in the Xiaolangdi Reservoir would have approximated to the erosion in the Sanmenxia Reservoir. That is, ~40% of the erosion in the Xiaolangdi Reservoir in 2019 (265 Mt) was attributable to natural floods, whereas ~60% was ascribed to drawdown and artificial floods. Specifically, the mean water inflow and outflow of the Xiaolangdi Reservoir during 22 June–12 July were 1760 and 3860 m³ s⁻¹, respectively, compared with 813 m³ s⁻¹ during the half year prior to 22 June (Fig. 2B). This suggested a moderate natural flooding and a severe drawdown-induced artificial flooding during the period from 22 June to 12 July. Based on the sediment budget of inflow and outflow, the cumulative erosion in the Xiaolangdi Reservoir during this 21-day period was 113 Mt (Fig. 2F), which undoubtedly should be attributed mainly to drawdown practices. Between 13 July and 10 August, the water level and water storage capacity were at their lowest, and less artificial flow was formed, which led to a high consistency between water outflow and inflow (Fig. 2B–C). During this period, a severe natural flooding with a highest water inflow of 4570 m³ s⁻¹ occurred, and the cumulative erosion amounted to 224 Mt (Fig. 2F). This rapid erosion should
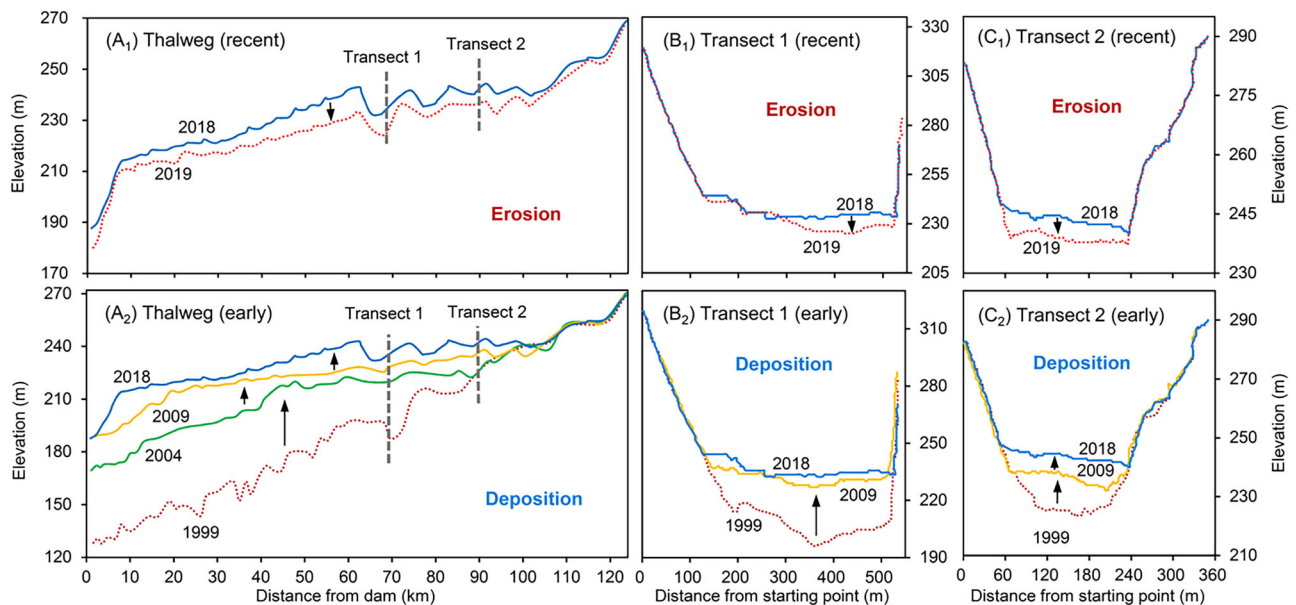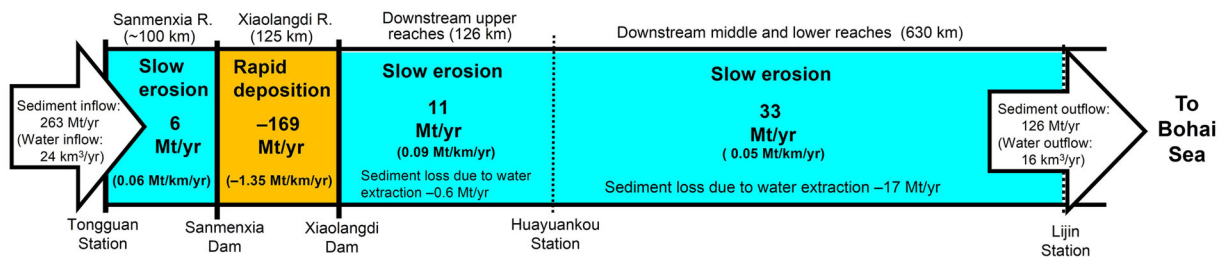
Fig. 6 | Deposition and erosion along a longitudinal section and two cross-sections in the Xiaolangdi Reservoir. A Temporal changes in the surface sediment profile along the thalweg. **B, C** Temporal changes in the profile along transects 1 and 2, respectively (see Fig. 6A for locations). Bathymetric surveys in each year were undertaken in October.
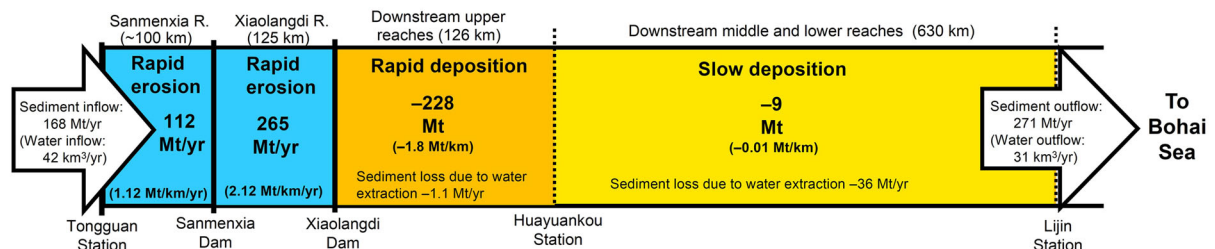

Fig. 7 | Sediment transport processes in the study area. Sediment flow, and erosion and deposition in the Sanmenxia (Sanmenxia R.) and Xiaolangdi (Xiaolangdi R.) reservoirs and downstream reaches of the Yellow River in (**A**) the period 1999-2018 and (**B**) 2019. Blue, erosion; brown, deposition; positive value, gain of sediment flow; negative value, loss of sediment flow; distance in parentheses = length of river reach.

be attributed to the combined effect of drawdown and natural flooding. After that, water impoundment practices were conducted, and a compensatory deposition amounting to ~70 Mt occurred, despite a second severe flooding. Therefore, in fully silted reservoirs, like the Sanmenxia Reservoir, considerable erosion will most likely occur during episodic natural flooding events[35], unless erosion has already occurred during previous floods. In half silted reservoirs (such as the Xiaolangdi Reservoir), erosion depends on the combination of natural floods with water management practices. Drawdown prior to natural flooding and maintaining lowest water level and storage during the flooding are effective practices to cause erosion. On the other hand, water impoundment during flooding will reduce erosion or even lead to deposition. Water regulation has been applied in many

reservoirs worldwide to reduce sedimentation and maintain storage capacity[20,28,36].

Our results of the case study from seven reservoirs indicate that the sedimentation ratio (sedimentation volume/storage capacity) at which initial annual net erosion occurs ranged from 28% to 87% with an average of 60% ± 21% (Table 1). Therefore, we propose a critical threshold of sedimentation ratio as ~30% to assist in assessing the risk of sediment erosion in reservoirs. Generally, a higher sedimentation ratio corresponds to an increased risk of reservoir erosion during floods. Compared to coastal sediments, sediments deposited in reservoirs are generally low in compaction and high in water content[37–39], because of rapid deposition of fine-grained particles in a short history. For example, the sedimentation histories

Article

prior to initial erosions in the seven reservoirs ranged from 5 to 20 years (Table 1). As shown in Supplementary Fig. S3, the overall dry bulk density of the sedimentation in the Sanmenxia and Xiaolangdi Reservoirs is 0.93 g cm^{-3}. In the Songtao Reservoir in South China, dry bulk density is only 0.61 g cm^{-3}[37]. In comparison, the dry bulk density of coastal sediments is generally 1.2–1.5 g cm^{-3}[38,39]. A lower critical shear stress for erosion is often related to a lower bulk density of relatively freshly deposited muddy sediments[40,41]. Consequently, reservoir sediments can be more susceptible to erosion when exposed to flowing water. Water depth in reservoirs decreases with siltation. In the Xiaolangdi Reservoir, for example, the channel bed level increased by more than 80 m at a location near the dam and by ~50 m in the middle reaches due to siltation from 1999 to 2018 (Fig. 6A$_2$), corresponding to a sedimentation ratio of 28%, prior to the initial erosion occurred in 2019 (Table 1). An increase in bed level means a decrease in cross-section of the river. Under a specific water inflow, it is expected that current velocity may increase in a channel where the cross-section has been reduced. In other words, the time that water inflow stays in a reservoir is proportional to the amount of water stored[15], so reduced water storage implies higher velocity of flow through the reservoir. The sediment-carrying capacity of flowing water is proportional to the cube of the flow velocity[42,43]. The water inflow of reservoirs during flood events can be several times greater than normal inflow (see Fig. 2A for examples). With not only much greater water inflow but also much higher flow velocity, the total sediment-carrying capacity would increase evidently in highly silted reservoirs during flood events. Drawdown-induced artificial flooding and water-depth decrease would further increase erosion in silted reservoirs. Thus, the sedimentation ratio for initial reservoir erosion may be associated with factors such as sediment compaction, grain-size distribution and hydrodynamic threshold, and the difference in this sedimentation ratio among reservoirs could be influenced by local conditions of meteorology, hydrology, sediment property, reservoir design, and even reservoir management.

Erosion depths of a few meters to >10 m during reservoir flushing events have been reported in previous studies. For example, erosion depths of 1.0–2.3 m along the mainstream in the Cachi Reservoir, Costa Rica, were surveyed during a 1-month flushing in 1996[44], and erosion depths of 4–14 m were measured in lakes Aldwell and Mills, USA, within 1 year of dam removal[22]. Flood–drawdown-induced episodic erosion in the Xiaolangdi Reservoir in 2019 yielded a maximum erosion depth of 11 m along the main channel, likely greater than that in most cases of episodic reservoir erosion, with >10% of previously deposited sediment being eroded with an increase in reservoir net storage capacity of 4–5%. Initial erosion in the Sanmenxia Reservoir during 1965 constituted 8% of the prior total deposition, and the maximum annual erosion in 1971 constituted 10% of prior net deposition (Fig. 4), increasing reservoir net storage capacity by 13% and 11%, respectively. Sediment outflow of the Xiaolangdi Reservoir during episodic erosion in 2019 increased by more than an order of magnitude compared with inflow (Fig. 2F). Outflow SSC levels from the Xiaolangdi Reservoir during 2019 episodic erosion events, with peak values of up to 210 kg m^{-3} and an event-averaged value of 57 kg m^{-3}, were higher than those recorded during many other episodic reservoir erosion events. For example, in a flushing operation in the Valgrosina Reservoir, Italy, the outflow SSC peaked at 80 kg m^{-3}, with an average of 4 kg m^{-3}[45]. Peak SSC values of 11–17 kg m^{-3} were recorded during dam-flushing events in the Arc–Isère River system, France[24]. Peak SSC values of 21–28 kg m^{-3} were recorded during flushing of reservoirs in the Kurobe River, Japan[20]. A maximum SSC of 850 kg m^{-3} was once recorded during breaching of the Condit Dam in the White Salmon River, USA[21], much higher than the peak SSC of 210 kg m^{-3} recorded in the Xiaolangdi Reservoir during 2019 episodic erosion events. In extreme cases, peak SSC levels during the flushing of reservoirs may exceed 1000 kg m^{-3}[28]. Episodic erosion in silted-up reservoirs can thus be very intense, with extremely turbid outflow.

Episodic reservoir erosion events may have severe ecological impacts in downstream reaches. Such erosion usually forms fluid mud with SSC levels exceeding 10 kg m^{-3}[46] in downstream river channels (Fig. 3B, C). Episodic

erosion of the Sanmenxia and Xiaolangdi reservoirs in 2019 led to the formation of fluid mud at Xiaolangdi Station (gauging outflow of the Xiaolangdi Reservoir) for 27 days (10 July-11 August, excluding 1 and 3–7 August, avg. SSC 69 kg m^{-3}) (Fig. 2E). At Huayuankou Station, 126 km downstream, fluid mud persisted for 32 days (11 July-13 August, excluding 5 and 12 August, avg. SSC 26 kg m^{-3}). Even at Lijin Station (tidal limit), 630 km farther downstream, fluid mud lasted 33 days (14 July-15 August, avg. SSC 18 kg m^{-3}), based on daily SSC data collected by the Yellow River Conservancy Commission (YRCC). These findings add to our previous understanding from other reservoirs worldwide that the initial period of erosion, with a duration ranging from a few hours to several days depending on the size of the reservoir, is characterized by extremely high SSC levels[24,28,45]. Due to the lack of specific ecological surveys, the environmental impact analysis in this study has certain limitations. Nevertheless, previous research has demonstrated related effects. High turbidity reduces photosynthesis in phytoplankton[47], thereby reducing primary productivity; and the combination of fluid mud, which smothers benthic organisms and clogs gills, and anoxia may kill virtually all organisms in a river[48,49]. Similar acute negative effects have been described for invertebrates[45]. Meanwhile, rapid deposition caused by extremely high SSC levels may destroy benthic communities where organisms tend to reside in the uppermost 10 cm of the sediment layer[50]; in many cases of episodic reservoir erosion, downstream channel deposition may exceed this threshold thickness[21,24,34]. Many natural reserves in the lower Yellow River and Yellow River Delta[51,52] would inevitably be affected by fluid mud and rapid deposition. Of course, to some extent, episodic reservoir erosion can alleviate the sediment starvation in estuarine deltas if it is well arranged[53].

Reservoir sediment erosion and its ecological impacts on downstream environments under episodic flooding and drawdown conditions have been reported in previous studies, either based on field measurements or numerical simulations[54–56]. Based on the sedimentation ratio of 30% proposed earlier in this study—above which reservoirs are at risk of erosion under episodic flooding and drawdown conditions—a map showing the global distribution of 57 large reservoirs (storage capacity > 0.1 km³) with more than 30% loss in capacity has been generated. Many reservoirs worldwide are fully or >30% silted-up, especially in the Northern Hemisphere, such as in China, India, Japan, United States and Iran (Fig. 8; Table 2). It indicates that episodic flooding and drawdown events may pose a widespread threat globally, and their impacts on the ecological environment of downstream river channels should not be overlooked. The lack of hydrological measurements and bathymetric surveys in most of the world's rivers[4] means episodic erosion in other silted-up reservoirs may remain undocumented. Perhaps the use of advanced GIS, geostatistical methods and remote sensing could be a good option to identify changes in topography and terrain in river drainage basins and networks during extreme events[57]. The above examples indicate that episodic erosion events in silted-up reservoirs during extreme floods and/or water-regulation periods may be common, with considerable impact on river sediment transport and fluvial environments. More reservoirs are being constructed or planned, particularly in developing countries such as China and Brazil[31], so it is expected that an increasing number of reservoirs will become silted up[58]. Moreover, extreme flooding will likely increase under global warming[59,60]. It follows that episodic erosion in reservoirs worldwide may become increasingly common and more intense in coming decades. Strengthening coordinated water regulation between upstream and downstream reservoirs and increasing water discharge during flood periods can help reduce SSC. This, in turn, can mitigate sediment deposition in downstream channels and the ecological impacts of turbid water, allowing more sediment to reach the estuarine delta and alleviating the ongoing erosion caused by sediment deficiency[35,49]. Considering the differences in reservoir function types (e.g., hydropower, water supply, and sediment-regulating reservoirs), reservoir morphology, sediment characteristics, hydrology, and geology, improvement of management practices (e.g., drawdown timing, water discharges) varies across reservoirs[54,61].
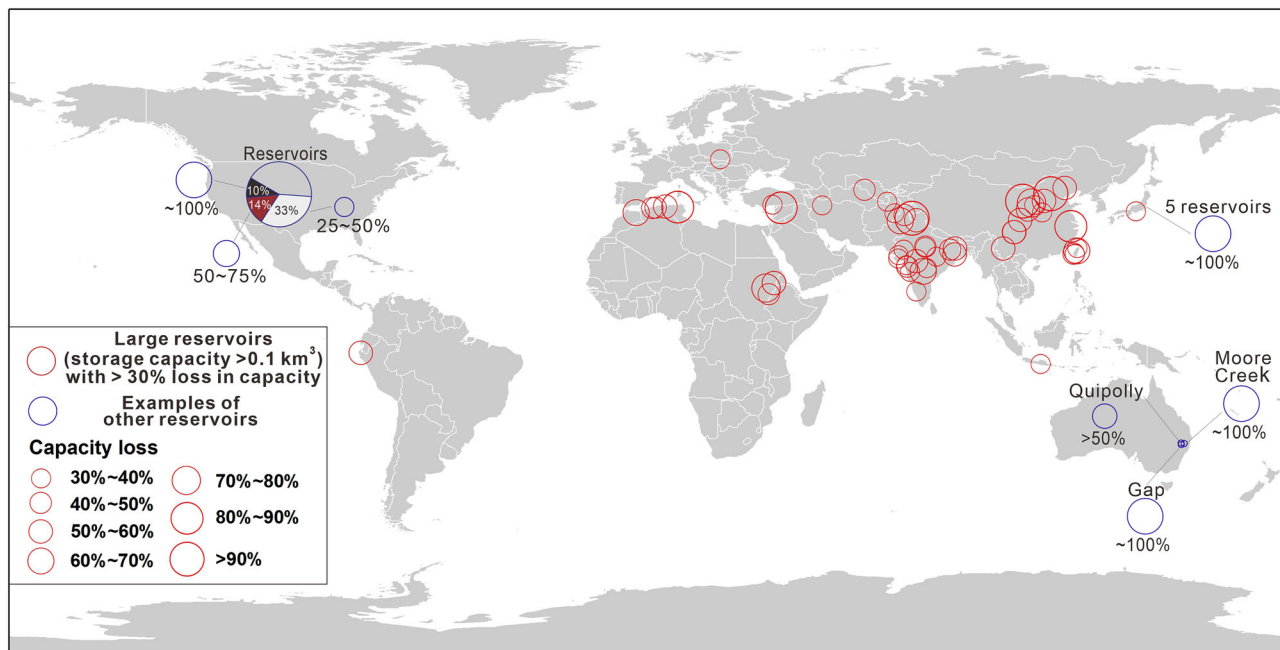
Fig. 8 | Global distributions of large reservoirs (storage capacity >0.1 km³) with > ³0% loss in capacity and examples of other severely silted-up reservoirs. This figure is created based on Minocha and Hossain[30] and Table 2.

Conclusions

Episodic reservoir erosion events and their downstream sedimentary impacts were identified on the basis of data for seven reservoirs in China. Maximum reservoir erosion depth may exceed 10 m during a flood event, increasing the downstream sediment load by one to two orders of magnitude, with peak SSC levels of up to 210 kg m⁻³. Sediment derived from reservoir erosion during a flood event may contribute not only most of the annual sediment flux, but also ~25% of the decadal sediment flux in downstream reaches. Threshold siltation ratios at which initial erosion occurred in the studied reservoirs were in the range of 28–87%, with such erosion occurring 5–26 years after impoundment. Natural floods alone can cause severe erosion in reservoirs, like the example of the Sanmenxia Reservoir where an erosion of 112 Mt was observed in the flooding 2019. However, regulated drawdown and artificial floods can effectively increase reservoir erosion during natural flooding events. ~60% of the Xiaolangdi erosion was attributed to drawdown and artificial flooding, whereas ~40% was attributed to natural floods. Our results indicate that episodic erosion can occur in partially silted reservoirs, with natural floods and regulation-induced low water depths providing favorable conditions. We supposed that the mechanisms responsible for reservoir erosion are that rapidly silted loose fine-grained sediments are easily erodible under high sediment-carrying capacities during flooding and drawdown. Reservoir erosion-induced extremely high SSC levels and related rapid deposition in downstream channels may adversely affect river ecosystems and socioeconomics. It is anticipated that reservoir erosion will become more frequent worldwide in the near future, as an increasing number of reservoirs will likely silt up, and the frequency of extreme floods may increase with global warming. Our findings aid understanding of the positive and negative effects of reservoirs on river systems, and may promote improvements in river management.

Methods
Study area

Seven large reservoirs in China were examined as case studies, including the Yanguoxia (0.23 km³ storage capacity; 36.2°N, 103.5°E), Qingtongxia (0.61 km³; 37.9°N, 106.3°E), Wanjiazhai (0.90 km³; 39.9°N, 111.5°E), Sanmenxia (6.0 km³; 35.1°N, 111.6°E), and Xiaolangdi (12.7 km³; 35.3°N, 113.2°E) reservoirs on the Yellow River; the Naodehai Reservoir (0.17 km³; 42.6°N, 121.5°E) on the Liuhe River; and the Gongzui Reservoir (0.31 km³; 28.8°N,

102.9°E) on the Daduhe River (Fig. 1A). Those on the Yellow River are located in downstream order along the mainstream of the Yellow River (Fig. 1B), which originates on the Qinghai–Tibet Plateau at 4200 m above sea level and flows 5460 km eastward to the Bohai Sea (Fig. 1B). The basin has a catchment area of 750,000 km² and currently supports a population of 110 million people. The average annual precipitation and potential evaporation within the Yellow River basin are 460 mm and 1700 mm, respectively. The water discharge and sediment flux from the Yellow River to the sea were 47 km³ yr⁻¹ and 1400 Mt yr⁻¹, respectively, prior to dam constructions, which begun in the 1960s[2,10,39] (Fig. 1C). Tongguan Hydrologic Station is commonly acknowledged as being the entrance to the Sanmenxia Reservoir[34,62]. Sanmenxia Station lies between the Sanmenxia Dam and the Xiaolangdi Reservoir, and Xiaolangdi Station is located immediately downstream of the Xiaolangdi Dam. Sanmenxia and Xiaolangdi stations are thus ideal for respectively gauging inflow and outflow of the Xiaolangdi Reservoir. Huayuankou Station is ~200 km downstream of Xiaolangdi Station, and Lijin Station (the tidal limit) a farther ~600 km downstream (Fig. 1A). The Liuhe River is a tributary of the Liaohe River[27,63], which is a major river in Northeast China with a length of 1345 km and a catchment area of 229,000 km², supporting a population of 35 million. Its water discharge and sediment flux to the sea were ~5 km³ yr⁻¹ and 40 Mt yr⁻¹, respectively, before declining in the 1960s[53,64]. The Daduhe River, SW China, is a secondary tributary of the Yangtze River[65], which is one of the world's largest rivers, with a length of 6400 km, a drainage area of 1.8 million km², 900 km³ yr⁻¹ of water discharge, and 500 Mt yr⁻¹ of sediment discharge prior to dam construction, supporting a population of 450 million[66].

Data source

Bathymetric data from the Sanmenxia and Xiaolangdi Reservoirs and water and sediment fluxes at the gauging stations along the Yellow River were compiled by the Yellow River Conservancy Commission (YRCC) of the Ministry of Water Resources of China (MWRC) (http://www.mwr.gov.cn). Sources of deposition/erosion data for other reservoirs were as follows: Qingtongxia Reservoir, changes in storage capacity reported by Li[67]; Yanguoxia Reservoir, Zhang[68]; Wanjiazhai Reservoir, Ren et al.[69]; Naodehai Reservoir, changes in storage capacity reported by Han[27] and Jiao et al.[63]; Gongzui Reservoir, Lin[65] for 1971–1986 and Xiong and Ma[70] for 1994–2007. All the available Sentinel-2 Level-2A and Landsat-8 Collection 2 Level-2

Table 2 | Examples of severely silted-up reservoirs worldwide

Reservoirs	Country	River (Tributary)	Operation period	Storage capacity (Mm³)	Capacity loss (%)	Sources
10% of reservoirs	USA	-	1920s–1970s	50,000	Nearly 100	Han[27]
Moore Creek	Australia	Moore Creek	1898–1924	0.22	Nearly 100	Chanson & James[74]
Gap	Australia	WerrisCreek	1902–1924	-	Nearly 100	Chanson & James[74]
5 reservoirs	Japan	-	1912–1972	-	Nearly 100	Han[27]
43 reservoirs	Shaanxi, China	-	1950s–1973	340	Nearly 100	Han[27]
Yuexijinshan	China	Hai	1961–1994	0.43	Nearly 100	Tian et al.[75]
20% of reservoirs	China	Yellow	–2015	Each > 0.5	Nearly 100	Wang et al.[76]
87% of reservoirs	China	Yellow	–2015	Each <0.5	Nearly 100	Wang et al.[76]
Qingtongxia	China	Yellow	1967–1998	606	96	Chen[77]
Zhangjiawan	China	Yellow (Qingshui)	1959–1964	119	85	Jiang & Fu[78]
Shuicaozi	China	Yili	1958–1981	9.6	85	Huang[79]
Yanguoxia	China	Yellow	1961–1998	232	82	Zhang et al.[80]
Zhenziliang	China	Yellow (Hun)	1959–1973	0.36	80	Jiang & Fu[78]
Xinqiao	China	Hongliu	1960–1973	200	75	Lin[65]
14% of reservoirs	USA	-	1920s–1970s	70,000	50–75	Han[27]
Tianqiao	China	Yellow	1973–1991	0.84	70	Liu et al.[81]
Sanba	China	Yangtze (Yuanshui)	1958–1998	0.11	68	Lu et al.[81]
Caizhuang	China	Yellow (Baima)	1960–1989	0.21	62	Tian et al.[75]; Liu et al.[81]
Bajiazui	China	Yellow (Pu)	1960–1972	257	61	Lin[65]
Toutunhe	China	Toutunhe	1971–1993	20	60	Chen et al.[82]
Manshan	China	Songhua	1978–1994	1.1	56	Tian et al.[75]
Dongxia	China	Yellow (Nan)	1959–1983	77	54	Tian et al.[75]; Jiang & Fu[78]
Miaogong	China	Hai	1960–1986	183	53	Tian et al.[75]
Tongjiezi	China	Yangtze (Daduhe)	1991–1998	210	52	Linghu[83]
Fenhe	China	Yellow (Fenhe)	1960–2005	721	52	Lin[65]; Liu[84]
Bikou	China	Yangtze (Bailong)	1975–1996	521	52	Yu[85]
Quipolly	Australia	Quipolly Creek	1932–1952	0.86	>50	Chanson & James[74]
Yumin	China	Yangtze (Jinshajiang)	1960–2000	8.0	50	Tian et al.[75]; Liu[86]
33% of reservoirs	USA	-	1920s–1970s	165,000	25–50	Han[27]
Sefid-Rud	Iran	Sefid-Rud	1963–1980	1,760	36	Morris & Fan[28]
Wonogiri	Indonesia	Bengawan Solo	1982–2011	730	33	Wulandari[87]

images with cloud cover <20% were acquired from the Google Earth Engine (GEE) platform for the period of 1 June to 31 August, 2019. Both datasets were spatially clipped to the study area boundary and exported as GeoTIFFs in WGS84 (EPSG:4326) at native resolution (10 m for Sentinel-2; 30 m for Landsat-8)[71]. Most data of global reservoir capacity and their losses in capacity were obtained from Minocha and Hossain[30].

Estimating water and sediment supply from ungauged areas
There is no gauging station in the 12,000 km² of tributaries between Tongguan and Xiaolangdi stations. To better understand erosion and deposition in this mainstem reach, we estimated water and sediment inflows that originated from the ungauged tributaries using an analogy method. There are three gauging stations, namely Hejin (catchment area of 38,700 km²), Heishiguan (catchment area of 18,600 km²), and Wuzhi (catchment area of 12,900 km²), on the tributaries, either higher than Tongguan Station or lower than Xiaolangdi Station (Fig. 1B). The ratio of the ungauged area (12,000 km²) to the total gauged area of these three stations (70,200 km²) is 0.171. Thus, we calculated water and sediment inflows from the ungauged tributaries as follows:

$$Q_{-ungauged(Tongguan-Xiaolangdi)} = 0.171(Q_{(Hejin)} + Q_{(Heishiguan)} + Q_{(Wuzhi)}) \tag{1}$$

where $Q_{-ungauged\ (Tongguan-Xiaolangdi)}$ represents the water inflow from the area of ungauged tributaries between Tongguan and Xiaolangdi Stations, and $Q_{(Hejin)}$, $Q_{(Heishiguan)}$, and $Q_{(Wuzhi)}$ are the water flows at Hejin, Heishiguan, and Wuzhi Stations, respectively, and

$$Q_{s-ungauged(Tongguan-Xiaolangdi)} = 0.171(Q_{s(Hejin)} + Q_{s(Heishiguan)} + Q_{s(Wuzhi)}) \tag{2}$$

where $Q_{s-ungauged\ (Tongguan-Xiaolangdi)}$ is the sediment inflow from the area of ungauged tributaries, and $Q_{s\ (Hejin)}$, $Q_{s\ (Heishiguan)}$, and $Q_{s\ (Wuzhi)}$ are the sediment flows at Hejin, Heishiguan, and Wuzhi Stations, respectively.

Quantifying deposition and erosion in reservoirs
The Sanmenxia and Xiaolangdi reservoirs began operating in September 1960 and October 1999, respectively[36,62]. For the period of 1960–1998, the sediment outflow that was subtracted from the sediment inflow for the reach between Tongguan and Xiaolangdi stations may have reflected mainly deposition (negative value indicates erosion) in the Sanmenxia Reservoir, assuming that deposition or erosion in the non-reservoir reach between the Sanmenxia Dam and Xiaolangdi Station was negligible. Thus, we calculated the annual weight of deposited sediment in the

Sanmenxia Reservoir as follows:

$$D_{(Weight\ in\ Sanmenxia\ Reservoir)} = Q_{s(Tongguan)} + Q_{s-ungauged(Tongguan-Xiaolangdi)} - Q_{s(Xiaolangdi)}$$

$$(3)$$

where $D_{(Weight\ in\ Sanmenxia\ Reservoir)}$ represents the annual weight of deposited sediment in the Sanmenxia Reservoir.

For the period of 1999–2020, the sediment outflow subtracted from the sediment inflow for the reach between Tongguan and Xiaolangdi stations reflects the net weight of deposited sediment in the Sanmenxia and Xiaolangdi reservoirs. Since 1999, annual volume of deposited sediments has been surveyed in the two reservoirs, using a bathymetric approach[34]. We calculated the total volume of deposited sediment as follows:

$$D_{(Total\ volume)} = D_{(Volume\ in\ Sanmenxia\ Reservoir)} + D_{(Volume\ in\ Xiaolangdi\ Reservoir)}$$

$$(4)$$

where $D_{(Total\ volume)}$ represents the total volume of deposited sediment, $D_{(Volume\ in\ Sanmenxia\ Reservoir)}$ represents the volume of deposited sediment in the Sanmenxia Reservoir, and $D_{(Volume\ in\ Xiaolangdi\ Reservoir)}$ is the volume of deposited sediment in the Xiaolangdi Reservoir.

Then, we calculated the total weight of deposited sediment in the two reservoirs as follows:

$$D_{(Total\ weight)} = Q_{s(Tongguan)} + Q_{s(Tongguan-Xiaolangdi)} - Q_{s(Xiaolangdi)} \quad (5)$$

Next, we made a double-mass plot of the cumulative volume of deposited sediment and cumulative weight of deposited sediment (Supplementary Fig. S3). This plot shows a strong correlation ($R^2 = 0.99$), suggesting that the annual deposition data obtained using the two approaches are highly credible. The plot also suggests an overall dry bulk density of $0.93\ g\ cm^{-3}$. Using this value, we converted the annual volume of deposited sediment to an annual weight of deposited sediment.

Finally, we adjusted the converted annual weight of deposited sediments based on the ratio of $D_{(Weight\ in\ Sanmenxia\ Reservoir)}$ to $D_{(Weight\ in\ Xiaolangdi\ Reservoir)}$ and the ratio of $D_{(Total\ weight)}$ to the sum of $D_{(Weight\ in\ Sanmenxia\ Reservoir)}$ and $D_{(Weight\ in\ Xiaolangdi\ Reservoir)}$, where $D_{(Weight\ in\ Sanmenxia\ Reservoir)}$ is the weight of deposited sediment in the Sanmenxia Reservoir, $D_{(Weight\ in\ Xiaolangdi\ Reservoir)}$ is the weight of deposited sediment in the Xiaolangdi Reservoir, and $D_{(Total\ weight)}$ is the total weight of deposited sediment in the two reservoirs calculated using the sediment-budget approach, following the principle that the sum of the adjusted $D_{(Weight\ in\ Sanmenxia\ Reservoir)}$ and $D_{(Weight\ in\ Xiaolangdi\ Reservoir)}$ is equal to $D_{(Total\ weight)}$.

Reporting summary
Further information on research design is available in the Nature Portfolio Reporting Summary linked to this article.

Data availability
The data used in this study are in Microsoft Excel format, which can be accessed at https://doi.org/10.6084/m9.figshare.28711874.v6[72].

References

1. Syvitski, J. P. M., Vörösmarty, C. J., Kettner, A. J. & Green, P. Impact of humans on the flux of terrestrial sediment to the global coastal ocean. *Science* **308**, 376–380 (2005).
2. Milliman, J. D. & Farnsworth, K. L. River discharge to the coastal ocean: A global synthesis. Cambridge: Cambridge University Press (2011).
3. Yang, H. F. et al. Human impacts on sediment in the Yangtze River: A review and new perspectives. *Global Planet Change* **162**, 8–17 (2018).
4. Dethier, E. N., Renshaw, C. E. & Magilligan, F. J. Rapid changes to global river suspended sediment flux by humans. *Science* **376**, 1447–1452 (2022).
5. Li, Y., Zhao, G., Allen, G. H. & Gao, H. Diminishing storage returns of reservoir construction. *Nat Commun* **14**, 3203 (2023).
6. Gao, G. et al. Dam regulation on extreme streamflow-sediment relationships along the Yangtze River Basin. *Sci Bull* **70**, 866–870 (2025).
7. Vörösmarty, C. J. et al. Anthropogenic sediment retention: major global impact from registered river impoundments. *Global Planet Change* **39**, 169–190 (2003).
8. Walling, D. E. Human impact on land-ocean sediment transfer by the world's rivers. *Geomorphology* **79**, 192–216 (2006).
9. Syvitski, J. P. M. et al. Sinking deltas due to human activities. *Nat Geosci* **2**, 681–686 (2009).
10. Wang, H. et al. Recent changes of sediment flux to the western Pacific Ocean from major rivers in East and Southeast Asia. *Earth-Sci Rev* **108**, 80–100 (2011).
11. Anthony, E. J. Patterns of Sand Spit Development and Their Management Implications on Deltaic, Drift-Aligned Coasts: The Cases of the Senegal and Volta River Delta Spits, West Africa. In: Randazzo et al. (Eds.) Sand and Gravel Spits. Springer, London (21–36) (2015).
12. Li, L. et al. Global trends in water and sediment fluxes of the world's large rivers. *Sci Bull* **65**, 62–69 (2020).
13. Yang, S. L. et al. Streamflow Decline in the Yellow River along with Socioeconomic Development: Past and Future. *Water* **12**, 823 (2020).
14. Giosan, L., Syvitski, J., Constantinescu, S. & Day, J. Protect the world's deltas. *Nature* **516**, 31–33 (2014).
15. Yang, S. L. et al. Downstream sedimentary and geomorphic impacts of the Three Gorges Dam on the Yangtze River. *Earth-Sci Rev* **138**, 469–486 (2014).
16. Tessler, Z. D. et al. Profiling risk and sustainability in coastal deltas of the world. *Science* **349**, 638–643 (2015).
17. Maloney, J. M. et al. Mississippi River subaqueous delta is entering a stage of retrogradation. *Mar Geol* **400**, 12–23 (2018).
18. Luan, H. L., Ding, P. X., Yang, S. L. & Wang, Z. B. Accretion-erosion conversion in the subaqueous Yangtze Delta in response to fluvial sediment decline. *Geomorphology* **2021**, 107682 (2021).
19. Zhu, Q. et al. Hidden delta degradation due to fluvial sediment decline and intensified marine storms. *Sci Adv* **10**, eadk1698 (2024).
20. Kondolf, G. M. et al. Sustainable sediment management in reservoirs and regulated rivers: experiences from five continents. *Earth's Future* **2**, 256–280 (2014).
21. Wilcox, A. C., O'Connor, J. E. & Major, J. J. Rapid reservoir erosion, hyper-concentrated flow, and downstream deposition triggered by breaching of 38 m tall Condit Dam, White Salmon River, Washington. *J Geophys Res Earth Surf* **119**, 1376–1394 (2014).
22. Randle, T. J., Bountry, J. A., Ritchie, A. & Wille, K. Large-scale dam removal on the Elwha River, Washington, USA: Erosion of reservoir sediment. *Geomorphology* **246**, 709–728 (2015).
23. Poeppl, R. E., Coulthard, T., Keesstra, S. D. & Keiler, M. Modeling the impact of dam removal on channel evolution and sediment delivery in a multiple dam setting. *Int J Sediment Res* **34**, 537–549 (2019).
24. Antoine, G., Camenen, B., Jodeaua, M., Némeryd, J. & Esteves, M. Downstream erosion and deposition dynamics of fine suspended sediments due to dam flushing. *J Hydrol* **585**, 124763 (2020).
25. Wu, X. et al. Mega-reservoir regulation: A comparative study on downstream responses of the Yangtze and Yellow rivers. *Earth-Sci Rev* **245**, 104567 (2023).
26. Zhao, C. H., Zhu, Z. H. & Zhou, D. Z. Worldwide Rivers and Dams. Beijing: China Water Conservancy and Hydroelectric Press (2000).
27. Han, Q. W. Reservoir sedimentation. Beijing: Science Press (2003).

28. Morris, G. L. & Fan, J. Reservoir sedimentation handbook: Design and management of dams, reservoirs, and watersheds for sustainable use. New York: McGraw-Hill companies (2010).

29. Schleiss, A. J., Franca, M. J., Juez, C. & De Cesare, G. Reservoir sedimentation. *J Hydraul Res* **54**, 595–614 (2016).

30. Minocha, S. & Hossain, F. GRILSS: opening the gateway to global reservoir sedimentation data curation. *Earth Syst Sci Data* **17**, 1743–1759 (2025).

31. Latrubesse, E. M. et al. Damming the rivers of the Amazon basin. *Nature* **546**, 363–369 (2017).

32. Westra, S., Alexander, L. V. & Zwiers, F. W. Global increasing trends in annual maximum daily precipitation. *J Clim* **26**, 3904–3918 (2013).

33. IPCC. In: V. Masson-Delmotte (Eds.), Climate change 2021: The physical science basis. Contribution of Working Group I to the Sixth Assessment Report of the Intergovernmental Panel on Climate Change. IPCC (2021).

34. Ministry of Water Resources of China (MWRC). China River Sediment Bulletin 2020. Beijing: China Water Resources and Hydropower Press (2021).

35. Wu, X. et al. Boosting riverine sediment by artificial flood in the Yellow River and the implication for delta restoration. *Mar Geol* **448**, 106816 (2022).

36. Wang, H. et al. Impacts of the dam-orientated water-sediment regulation scheme on the lower reaches and delta of the Yellow River (Huanghe): A review. *Global Planet Change* **157**, 93–113 (2017).

37. Lu, G., Li, Y., Cai, F. & Wang, C. Research on the sedimentation of Songtao Reservoir, Hainan Island. *Trop Geogr* **5**, 157–167 (1985).

38. Yao, R., Yang, J. & Liu, G. Spatial variability of soil bulk density in the Yellow River Delta. *J Irrig Drain* **25**, 11–15 (2006).

39. Yang, S. L. et al. Role of delta-front erosion in sustaining salt marshes under sea-level rise and fluvial sediment decline. *Limnol Oceanogr* **65**, 1990–2009 (2020).

40. Taki, K. Critical shear stress for cohesive sediment transport. In: McAnally, W. H. & Mehta, A. J. (Eds.), Coastal and Estuarine Fine Sediment Processes. Elsevier Science, 53–61 (2001).

41. Zhu, Q. et al. The heterogeneity of mudflat erodibility. *Geomorphology* **345**, 106834 (2019).

42. Velikanov, M. A. Gravitational theory of sediment transport. *J Sci Soviet Union Geophys* **4**, 349–359 (1954).

43. Li, R., Dong, D., Zheng, J., Zhang, W. & Pan, X. Vertical suspended diffusion and nearshore sediment-carrying capacity theory. *Acta Oceanol Sin* **33**, 169–173 (2012).

44. Brandt, S. A. & Swenning, J. Sedimentological and geomorphological effects of reservoir flushing: the Cachi reservoir, Costa Rica, 1996. *Geogr Ann A* **81**, 391–407 (1999).

45. Crosa, G., Castelli, E., Gentili, G. & Espa, P. Effects of suspended sediments from reservoir flushing on fish and macroinvertebrates in an alpine stream. *Aquat Sci* **72**, 85–95 (2010).

46. Kineke, G. C., Sternberg, R. W., Trowbridge, J. H. & Geyer, W. R. Fluid-mud processes on the Amazon continental shelf. *Cont Shelf Res* **16**, 667–696 (1996).

47. Jewson, D. H. & Taylor, J. A. The influence of turbidity on net phytoplankton photosynthesis in some Irish lakes. *Freshwater Biol* **8**, 573–584 (1978).

48. Garric, J., Migeon, B. & Vindimian, E. Lethal effects of draining on brown trout. a predictive model based on field and laboratory studies. *Water Res* **24**, 59–65 (1990).

49. Newcombe, C. P. & MacDonald, D. D. Effects of suspended sediments on aquatic ecosystems. *North Am J Fish Manage* **11**, 72–82 (1991).

50. Shi, B., Yang, S. L., Temmerman, S. & Bouma, T. Effect of typhoon-induced intertidal-flat erosion on dominant macrobenthic species (Meretrix meretrix). *Limnol Oceanogr* **66**, 4197–4209 (2021).

51. Cui, B., Yang, Q., Yang, Z. & Zhang, K. Evaluating the ecological performance of wetland restoration in the Yellow River Delta, China. *Ecol Eng* **35**, 1090–1103 (2009).

52. He, X., Hrmann, G., Strehmel, A., Guo, H. & Fohrer, N. Natural and anthropogenic causes of vegetation changes in riparian wetlands along the lower reaches of the yellow river, china. *Wetlands* **35**, 391–399 (2015).

53. Wu, Z. et al. Anthropogenic impacts on the decreasing sediment loads of nine major rivers in China, 1954–2015. *Sci Total Environ* **739**, 139653 (2020).

54. Schenk, L. & Bragg, H. Sediment transport, turbidity, and dissolved oxygen responses to annual streambed drawdowns for downstream fish passage in a flood control reservoir. *J Environ Manage* **295**, 113068 (2021).

55. Artruc, T., Tullos, D. & Leshchinsky, B. Effects of drawdown scenario on retrogressive lateral erosion in a reservoir. *J Am Water Resour Assoc* **59**, 86–106 (2023).

56. Nikeghbali, P., Benjankar, R. & Kheirkhahan, M. Erosion under drawdown flushing with the SPH method. *Ocean Eng* **310**, 118743 (2024).

57. Valjarević, A. GIS-Based Methods for Identifying River Networks Types and Changing River Basins. *Water Resour Manage* **38**, 5323–5341 (2024).

58. Basson, G. R. Management of siltation in existing and new reservoirs. 23rd Congress of the International Commission on Large Dams (2009). 63

59. Roudier, P. et al. Projections of future floods and hydrological droughts in Europe under a +2°C global warming. *Clim Change* **135**, 341–355 (2016).

60. Zhang, W. & Zhou, T. Increasing impacts from extreme precipitation on population over China with global warming. *Sci Bull* **65**, 243–252 (2020).

61. Lewis, A. S. et al. Reservoir drawdown highlights the emergent effects of water level change on reservoir physics, chemistry, and biology. *J Geophys Res Biogeosci* **129**, e2023JG007780 (2024).

62. Hou, S. Z., Gou, X. J. & Hu, T. Influence of operation water level on deposition distribution in Sanmenxia Reservoir. *J Sediment Res* **44**, 14–18 (2019).

63. Jiao, E. Z., Zhang, Q. & Liu, Y. Operation and sedimentation pretention of Naodehai Reservoir. *Yellow River* **34**, 26–29 (2012).

64. Dai, S. B., Yang, S. L. & Li, M. Sharp decrease in suspended sediment supply from China's rivers to the sea: Anthropogenic and natural causes. *Hydrol Sci J* **54**, 135–146 (2009).

65. Lin, C. K. Characteristics nd sediment deposition in Gongzui Reservoir of the Daduhe River. *J Lake Sci* **4**, 11–18 (1992).

66. Yang, S. et al. Storms dominate the erosion of the Yangtze Delta and southward sediment transport. *Sci Bull* **68**, 553–556 (2023).

67. Li, T. Sedimentation in the Qingtongxia Reservoir. Dam and Security, 21–27 (1998).

68. Zhang, Y. Sedimentation in the Yanguoxia Reservoir based on measurements. Dam and Security, 14–21 (1999).

69. Ren, Z., Wang, T. & Qu, S. Sedimentation in the Wanjiazhai Reservoir. Proceedings of China Dam Engineering Society, 155–160 (2018).

70. Xiong, M. & Ma, W. Recent deposition in the Gongzui Reservoir. *Sichuan Water Power* **27**, 82–86 (2008).

71. Chen, C., Zhang, C., Tian, B., Wu, W. & Zhou, Y. Mapping intertidal topographic changes in a highly turbid estuary using dense Sentinel-2 time series with deep learning. *ISPRS J Photogramm Remote Sens* **205**, 1–16 (2023).

72. Yang, H. F. Data and the figures. figshare. Dataset. https://doi.org/10.6084/m9.figshare.28711874.v6 (2025).

73. Jia, E. The analysis of souring and sedimentation in Qingtongxia Reservoir. Master's thesis of the Xi'an University of science and Technology (2002).

74. Chanson, H. & James, P. Rapid Reservoir Sedimentation of Four Historic Thin Arch Dams in Australia. *J Perform Constr Fac* **12**, 85–92 (1999).

75. Tian, H. T., Zhang, Z. K. & Li, Y. M. Differences in reservoir sedimentation in Inland China. *Adv Sci Technol Water Resour* **26**, 28–33 (2006).

76. Wang, S. et al. Reduced sediment transport in the Yellow River due to anthropogenic changes. *Nat Geosci* **9**, 38–41 (2016).

77. Chen, G. Deposition in the Qingtongxia Reservoir and design of sediment release. *Mech Elect Inform* **605**, 142–143 (2019).

78. Jiang, N. & Fu, L. Problems of reservoir sedimentation in China. *J Lake Sci* **9**, 1–8 (1997).

79. Huang, G. S. On silt clearance in the Shuicaozi Reservoir. *J North China Inst Water Conserv Hydroelect Power* **22**, 87–89 (2001).

80. Zhang, W. et al. Spatio-temporal variation of the suspended sediment concentration in the Pearl River Estuary observed by MODIS during 2003–2015. *Cont Shelf Res* **172**, 22–32 (2019).

81. Liu, X. W., Zhang, J. J. & Cao, Z. Sedimentation in the Caizhuang Reservoir and countermeasures. *Sanxi Hydro Technics* **112**, 49–53 (1996).

82. Chen, Y., Chen, L. & Li, W. Analysis of silting of reservoirs in the Tianshan mountain area: Given the Toutunhe Reservoir as an example. *J Arid Land Resour Env* **10**, 46–51 (1996).

83. Linghu, K. On the sedimentation in the Tongjiezi Reservoir. *Sichuan Water Conserv* **21**, 28–33 (2000).

84. Liu, G. Gray prediction model of sedimentation in the Fenhe Reservoir. *J Hydraul Eng* **6**, 56–60 (1989).

85. Yu, G. L. Research on sediment silting and operation of the Bikou Reservoir. *J Hydroelect Eng* **64**, 59–67 (1999).

86. Liu, Y. On the sedimentation in the Yumin Reservoir. *Sichuan Water Conserv* **19**, 21–24 (1998).

87. Wulandari, D. A., Legono, D. & Darsono, S. Evaluation of deposition pattern of Wonogiri Reservoir sedimentation. *Int J Civ Eng* **15**, 1–6 (2015).

Acknowledgements

Author contributions

H.Y. and S.Y. contributed to conceptualization, project administration, writing-original draft, review and editing, M.T., B.S. and C.C. contributed in data curation, methodology and visualization, and H.W. contributed to project administration, supervision, and review and editing.

Competing interests

The authors declare no competing interests.

Additional information

Supplementary information The online version contains supplementary material available at https://doi.org/10.1038/s43247-025-02666-7.

Correspondence and requests for materials should be addressed to Shilun Yang.

Peer review information *Communications Earth & Environment* thanks Alejandro Mendoza and the other, anonymous, reviewer(s) for their contribution to the peer review of this work. Primary Handling Editors: Shan Liu and Alireza Bahadori. A peer review file is available.

Reprints and permissions information is available at http://www.nature.com/reprints

Publisher's note Springer Nature remains neutral with regard to jurisdictional claims in published maps and institutional affiliations.